

Human serum albumin and quercetin interactions monitored by time-resolved fluorescence: evidence for enhanced discrete rotamer conformations

Olaf J. Rolinski
Andrew Martin
David J. S. Birch

University of Strathclyde
Scottish Universities Physics Alliance
Photophysics Group
Department of Physics
John Anderson Building
107 Rottenrow
Glasgow G4 0NG, United Kingdom

Abstract. Human serum albumin (HSA) complexation with quercetin, a flavonoid commonly present in human diet, was monitored by means of fluorescence decays of the single HSA tryptophan - Trp214. Data analysis based on fitting to multiexponential functions and determining the lifetime distributions revealed a high sensitivity of tryptophan fluorescence to binding quercetin. Results are discussed in terms of the rotamer model for tryptophan, HSA-quercetin complexation and potential HSA to quercetin energy transfer. Evidence for quercetin stabilising tryptophan rotamers in HSA is presented. © 2007 Society of Photo-Optical Instrumentation Engineers. [DOI: 10.1117/1.2747623]

Keywords: human serum albumin; tryptophan rotamers; flavonoids; fluorescence lifetime distribution; fluorescence resonance energy transfer; quercetin.

Paper 06307RR received Oct. 30, 2006; revised manuscript received Feb. 28, 2007; accepted for publication Feb. 28, 2007; published online Jun. 15, 2007.

1 Introduction

There is increasing optimism that nanoscience applied to medicine will bring significant advances in diagnosis, e.g., presymptom disease monitoring, and will enable the use of preventative medicines at an early stage. One of the techniques that show much promise in this field is fluorescence, with its ability to offer noninvasive sensing by using light and its sensitivity to molecular events occurring on the nanometer scale. Sensing based on intrinsic fluorophores like the amino acids tryptophan and tyrosine has been widely investigated and offers full noninvasiveness, as the biomolecular systems are not perturbed by any extrinsic fluorophores such as those proposed for glucose sensing.¹⁻³

In this work, we focus on flavonoids, components of human diet associated with a number of biological activities in the human body, many of which can contribute to the prevention of disease. Fluorescence research on flavonoids to date,⁴⁻¹⁰ mostly steady state, demonstrates a unique environment-sensitive fluorescence of some flavonoids and their specific binding to proteins, DNA, and biomembranes. This makes flavonoids potential alternatives to fluorescent amino acids for noninvasive sensing.^{4,5} On many occasions they can play the roles of an analyte and fluorescence sensor simultaneously.

Flavonoids occur in many plants of higher genera, i.e., vegetables, fruits, and their products, e.g., teas, red wine, chocolate. In nature they regulate plant growth, inhibit or kill many bacteria strains, inhibit viral enzymes, e.g., transcriptase and protease, and destroy some pathogenic protozoans.^{4,5} The beneficial therapeutic role of flavonoids was already recognised in the 1930's,⁶ but in the past two decades interest in

therapeutically active flavonoids has undergone a remarkable renaissance due to their antioxidant role in a wide range of diseases like cancers, tumors, allergies, AIDS, and different free-radical-mediated disorders (e.g., atherosclerosis, ischemia, neuronal degeneration, and cardiovascular ailments).⁷

Most of the pharmacological actions of flavonoids are caused by their binding to biomolecular targets and causing alterations in their structures and functions. These interactions have been monitored by means of the steady-state fluorescence of the bound flavonoid,^{8,9} or by altering fluorescence of the fluorogenic target.^{10,11} For example, it has been found that the flavone fisetin⁵ binds DNA, which triggers excited-state proton transfer (ESPT) and results in increased tautomeric emission, proving that fisetin is localized in a hydrophobic environment. It has been also shown that the mechanism of binding is intercalative, as ethidium bromide replaces fisetin from its binding site in DNA in a competitive manner. On binding to human serum albumin (HSA), fisetin also shows tautomer emission, and fluorescence resonance energy transfer (FRET) from tryptophan to fisetin is observed for the excitation at 280 nm, suggesting close proximity between molecules.⁸ Other flavones, like quercetin,⁹ morin, or myricetin, also demonstrate strongly enhanced fluorescence on binding to specific proteins, e.g., bovine serum albumin (BSA) or insulin. Tryptophan fluorescence quenching was used¹⁰ to monitor interactions between BSA and catechin, epicatechin, rutin, and quercetin. The steady-state measurements suggested mixed static and collisional quenching. Similar experiment with HSA¹¹ confirmed formation of a ground-state complex, but also revealed influence of transition metal ions on flavonoid-protein complex formation.

Affinity of flavonoids to protein, together with the natural fluorescence of both, enable opportunities for noninvasive monitoring of their mutual interactions. In this research we

Address all correspondence to Olaf Rolinski Physics, University of Strathclyde, John Anderson Building - 107 Rottenrow, Glasgow, Scotland G4 0NG United Kingdom; Tel: +44-(0)-141-548-4230; Fax: +44-(0)-141-552-2891; E-mail: o.j.rolinski@strath.ac.uk

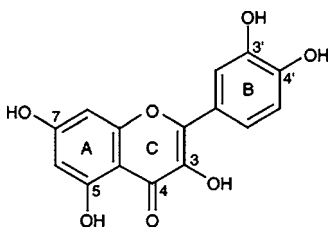


Fig. 1 Molecular structure of quercetin.

used HSA as a model protein. HSA is the most abundant of the proteins in the blood plasma and acts as a transport carrier of endogenous and exogenous ligands poorly soluble in water (e.g., some drugs, fatty acids, etc.). It can be easily bound by a number of flavonoids, including quercetin (see Fig. 1) used in these studies.

HSA is composed of several mostly helical domains that are structured by 17 disulfide bridges.¹² In particular, subdomains IIA and IIIA are delimited by a hydrophobic surface on one side and a positively charged surface on the other side, which allow them to specifically bind negatively charged heterocyclic ligands of average size and small aromatic carboxylic acids, respectively.¹² The only tryptophan (Trp 214) in HSA is part of the subdomain IIA. HSA contains also 18 tyrosines (Tyr) distributed throughout the protein at distances short enough to enable mutual Tyr→Tyr or Tyr→Trp FRET, but Trp→Tyr energy transfer is very unlikely due to poor spectral overlap between Trp emission and Tyr absorption spectra.

As HSA and Q in a complex are both fluorescent, their interactions can be monitored by means of three types of experiments (Fig. 2): excitation of HSA and detection of its fluorescence [Fig. 2(a)], excitation of Q and detection of Q fluorescence [Fig. 2(b)], and possibly, excitation of HSA and detection of fluorescence of Q as a result of FRET from Trp 214 in HSA to Q [Fig. 2(c)]. All three approaches, based on steady-state and lifetime measurements, were attempted in this work to give complementary information on the excited-state kinetics and thus the flavonoid-protein interactions.

2 Experimental

2.1 Sample Preparation

Quercetin dihydrate and HSA were purchased from Sigma-Aldrich and used without further purification. Buffered water

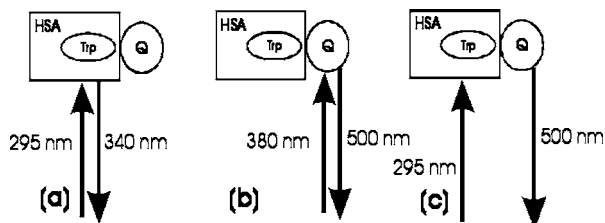


Fig. 2 Three potential channels of gaining information on HSA-Q interaction: (a) excitation and detection of tryptophan, (b) excitation and detection of flavonoid, and (c) excitation of HSA and detection of flavonoid. The pulsed sources wavelengths and the detection monochromator settings used in these studies are also shown.

solutions (0.01-M phosphate buffer, pH 7.4) of 30- μ M quercetin with varying concentrations of HSA (0 to 60 μ M) and of 30- μ M HSA with varying concentrations of quercetin (0 to 60 μ M) were prepared on the day of measurement.

2.2 Steady-State Measurements

The steady-state measurements were performed using a Perkin-Elmer (Beaconsfield, UK) Lambda 2 UV/VIS spectrometer for absorption and a Perkin-Elmer LS-50 B luminescence spectrometer for fluorescence spectra. Quercetin fluorescence was also probed by a Horiba Jobin Yvon (Stanmore, UK) SkinSkan spectrometer specially designed to enable front-face excitation as encountered in medical sensing.

2.3 Time-Resolved Measurements

The time-correlated single-photon counting technique (TCSPC) was used to record the fluorescence decays. The IBH 5000U fluorescence lifetime system (Horiba Jobin Yvon IBH Limited, Glasgow, UK), equipped with a choice of nanoLEDs emitting \sim 600 ps (fwhm) pulses at 279 nm,¹³ 295 nm,¹⁴ or 265 nm¹⁵ with the repetition rate of 1 MHz, was ideal for exciting fluorescence of amino acids in proteins. The time calibration of the system was 7.06 ps/channel.

In the TCSPC technique, the fluorescence decay function $I(t)$ is related to the experimental decay function $F(t)$ by the convolution integral

$$F(t) = \int_0^t L(t')I(t-t')dt', \quad (1)$$

where $L(t)$ is an excitation pulse profile. Two methods of deconvolution were used to reveal $I(t)$. 1. Fitting to a multi-exponential function using the least-squares method (DAS 6 package from Horiba Jobin Yvon IBH Limited). $I(t)$ was expressed as an analytical function with some unknown parameters. $I(t)$ was convoluted with the excitation pulse profile $L(t)$ and then compared with the experimental decay function $F(t)$ in terms of the χ^2 goodness-of-fit criteria. The best-fit parameters of $I(t)$ were found by minimizing the χ^2 functions. This approach was extensively used and proved its usefulness in recovery of the relatively simple decays (1- to 3-exponential, collisional quenching, Förster FRET). 2. On many occasions biological samples demonstrate fluorescence decays too complex to be expressed by analytical formula, and it is helpful to represent $I(t)$ as

$$I(t) = \int_0^\infty \exp[-t/\tau]g_D(\tau)d\tau, \quad (2)$$

and determine the fluorescence lifetime distribution function $g_D(\tau)$ using the maximum entropy method (MEM).¹⁶

This method (Pulse 5 procedure from Maximum Entropy Data Consultants Limited, Bury St. Edmunds, UK) recovers the $g_D(\tau)$ function and is ideal for representing $I(t)$ in a model-free form. However, the applicability of this model-free deconvolution is limited to the fluorescence decays that have no rise time. This limit results from the nature of the $g_D(t)$, which, as the distribution function, cannot be negative.

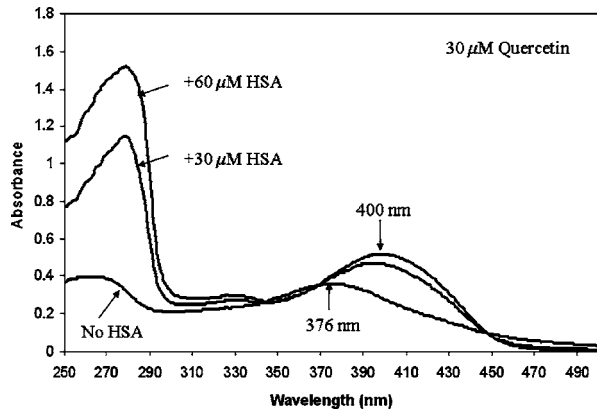


Fig. 3 The absorption spectra of the solutions containing 30- μM quercetin and 0, 30, and 60 μM of HSA.

3 Results and Discussion

3.1 Absorption and Fluorescence Spectra

Figure 3 presents the absorption spectra of quercetin in a buffer solution, without and with HSA. Free quercetin (30 μM) shows absorption peaks at 270, 325, and 376 nm. The addition of HSA (30 μM) results in enhanced absorption of quercetin, with the peaks at 325 and 376 nm shifted to about 328 and 400 nm, respectively. Similar results were obtained in earlier studies.¹⁷ Further increase of HSA level (up to 60 μM), increases the absorption peak at 400 nm only slightly. These observations are a first indication of the potential HSA-quercetin complex formation. Although there is possible indication of an isosbestic point in Fig. 3, further investigations suggest there is none, probably because three species, namely HSA, quercetin, and HSA-quercetin complex, are contributing to the absorption spectrum.

The interaction was further investigated by steady-state measurements of the solutions containing fixed amounts of HSA (30 μM) and varying concentrations of quercetin (0 to 60 μM) (Fig. 4). The sample with the lowest concentration of quercetin (10 μM) exhibits a maximum in the absorption spectra at 400 nm. Increasing the content of quercetin results

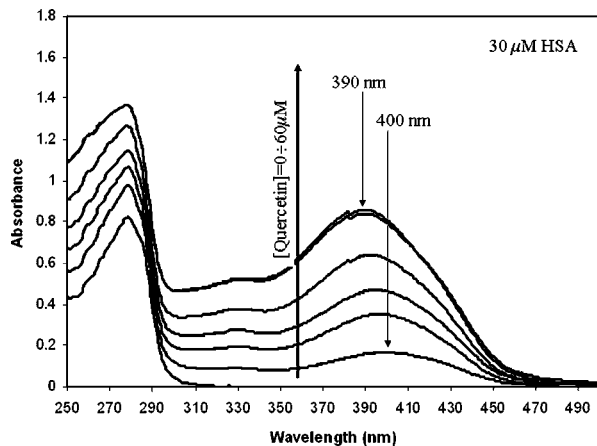


Fig. 4 The absorption spectra of the solutions containing 30- μM HSA and increasing (0–60 μM) concentrations of quercetin.

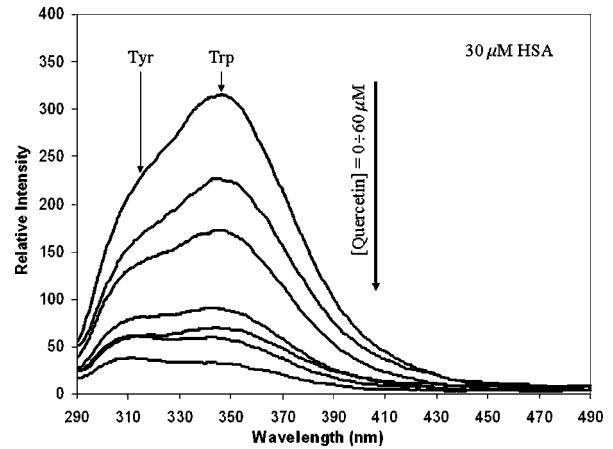


Fig. 5 Fluorescence spectra of 30- μM HSA with varying concentrations of quercetin, excited at 279 nm.

in stronger absorption, but also a shift of the spectra toward shorter wavelengths is observed, with the peak achieving 390 nm for 60 μM of quercetin. It suggests that for the $[\text{quercetin}] < [\text{HSA}]$, we observe the absorption of the HSA-quercetin complex only, while for $[\text{quercetin}] > [\text{HSA}]$, the absorption of free quercetin is also present.

Fluorescence spectra were measured for two different excitation wavelengths, namely 279¹³ and 295¹⁴ nm. The excitation at 279 nm, which fits better to the absorption maximum of the HSA (see Fig. 4), resulted in the spectra shown on Fig. 5. In the absence of quercetin, the HSA fluorescence is dominated by tryptophan (~ 340 nm) with some contribution of tyrosine (~ 315 nm). Fluorescence of both amino acids gradually decreases with increasing amounts of quercetin, with tryptophan fluorescence decreasing much faster. Finally, for a quercetin level of 60 μM , tyrosine fluorescence dominates. This result indicates some kind of quenching of tyrosine and tryptophan fluorescence by quercetin and that the tryptophan quenching is much more efficient. The last observation suggests that the quercetin binding site is close to the tryptophan.

The other conclusion, which can be drawn from Fig. 5, is that using the 279-nm nanoLED in lifetime measurements would be expected to result in complex fluorescence decays, as they would reflect kinetics involving tyrosine, tryptophan, and quercetin. Selective excitation of tryptophan by using the 295-nm nanoLED can offer more clear information on the interaction between tryptophan and quercetin, as the tyrosine absorption of this wavelength is low and the contribution of tyrosine to the kinetics is minimized. This is illustrated by Fig. 6, showing HSA fluorescence excited at 295 nm, quenched by quercetin. The spectra do not show a contribution from tyrosine. An inset shows a magnified 450- to 550-nm section of the spectra, showing very weak fluorescence of quercetin, which provides evidence of some FRET, as tryptophan does not emit in this spectral region. Indeed, the spectral overlap between the absorption spectrum of the quercetin-HSA complex and the fluorescence spectrum of the Trp214 results in the critical transfer distance $R_0 \cong 24 \text{ \AA}$,¹⁸ suggesting the contribution of FRET to the total kinetics.

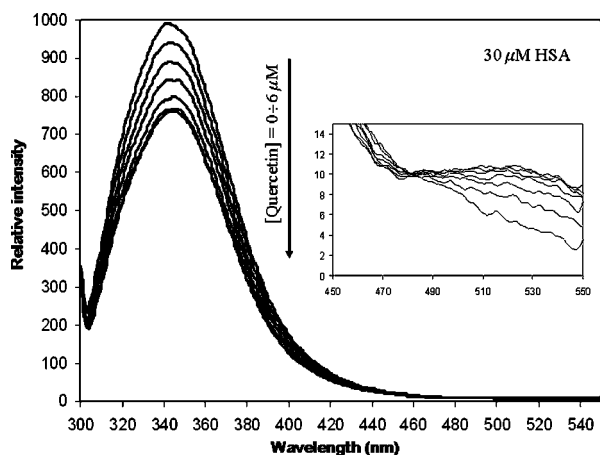
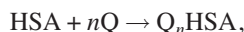


Fig. 6 Fluorescence spectra of 30- μ M HSA with varying concentrations of quercetin, excited at 295 nm. An inset shows an increased fluorescence in the region 490 to 550 nm, which is consistent with FRET from HSA to quercetin.

3.2 Quercetin: Human Serum Albumin Ratio

The Q:HSA ratio in the HSA-Q complex was established on the basis of the steady-state spectra. It was assumed that the complexation of HSA with quercetin occurs according to the equation



where n is a number of Q-binding sites on the HSA molecule. The total concentration of HSA, $[\text{HSA}_t]$, is the sum of the concentrations of the bound $[\text{Q}_n\text{HSA}]$ and free $[\text{HSA}_f]$ albumin.

$$[\text{HSA}_t] = [\text{HSA}_f] + [\text{Q}_n\text{HSA}]. \quad (3)$$

The relevant binding constant K_Q is defined as

$$K_Q = \frac{[\text{Q}_n\text{HSA}]}{[\text{Q}]^n[\text{HSA}_f]}, \quad (4)$$

thus

$$K_Q = \frac{[\text{HSA}_t] - [\text{HSA}_f]}{[\text{Q}]^n[\text{HSA}_f]}. \quad (5)$$

After rearrangements,

$$\frac{[\text{HSA}_t]}{[\text{HSA}_f]} - 1 = K_Q[\text{Q}]^n. \quad (6)$$

As the intensity of fluorescence $F \sim [\text{HSA}_f]$, and, for an albumin only, $F_0 \sim [\text{HSA}_t]$, the concentration ratio in Eq. (6) can be replaced by F_0/F , and finally

$$(F_0 - F)/F = K_Q[\text{Q}]^n. \quad (7)$$

As Fig. 7 shows, the linear dependence of $(F_0 - F)/F$ versus $[\text{Q}]^n$, was obtained for $n = 1.31$. The prior result is consistent with the 1:1 $[\text{HSA}]:[\text{quercetin}]$ ratio. However, exact interpretation of the received number may indicate that in about 2/3 of complexes, one HSA molecules is bound by one quercetin

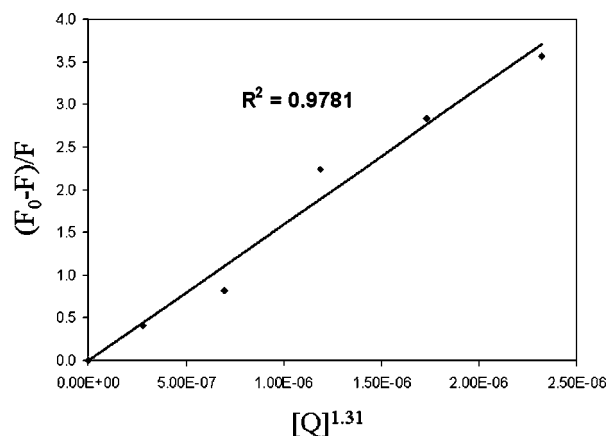


Fig. 7 Quercetin:HSA ratio plot. The n value resulting in linearity of the $(F_0 - F)/F$ versus $[\text{Q}]^n$ plot was found to be 1.31.

molecule, while in the remaining 1/3 of them, one HSA molecule is bound by two quercetin molecules. The estimated value of K_q is $(7.6 \pm 0.8) \times 10^4 \text{ M}^{-1}$.

3.3 Direct Excitation of Quercetin in Human Serum Albumin and Quercetin Complex

HSA-quercetin interactions were probed by means of the scheme shown in Fig. 2(b) by direct excitation of quercetin at 373 nm and detection of fluorescence spectra. Figure 8 shows results obtained using a SkinSkan spectrometer, which uses fiber optics and front-face excitation, practical for *in-vivo* sensing. In spite of a low concentration of quercetin, the spectra were easily measurable, which makes quercetin potentially useful in noninvasive transdermal sensing applications.

In the absence of HSA, a weak fluorescence with two peaks at 430 and 535 nm was found (Fig. 8). Addition of HSA results in enhancement of quercetin fluorescence and small shifts of the peaks to 445 and 545 nm, respectively. However, for $[\text{quercetin}] > [\text{HSA}]$, the longer wavelength peak tends to return to its previous position (535 nm), indicating some contribution of the free-quercetin fluorescence. The characteristic dual fluorescence of quercetin observed here can be attributed to two emitting forms of quercetin: a normal form (band with the peak at 430 nm) and the ESPT form

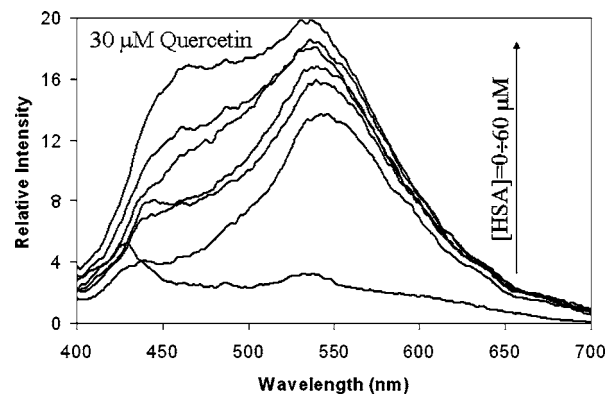


Fig. 8 Fluorescence spectra of quercetin with varying concentrations of HSA excited at 373 nm.

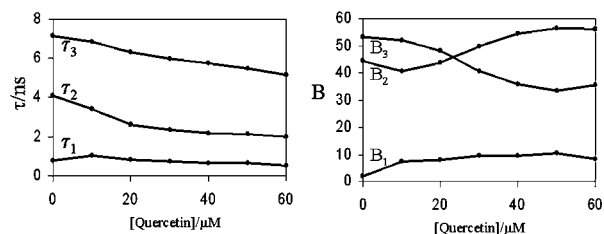


Fig. 9 Lifetime data by means of three-exponential decays. Fluorescence decays were fitted to $I(t) = A + b_1 \exp[-t/\tau_1] + b_2 \exp[-t/\tau_2] + b_3 \exp[-t/\tau_3]$. The plot presents the percentage contribution of each component, namely $B_i = b_i \tau_i / \sum b_j \tau_j$.

(545 nm).¹⁹ The intensity ratio of the tautomer to normal fluorescence decreases with increasing concentration of HSA, until $[HSA][quercetin] \sim 1$, and then it tends to level off. This suggests that ESPT in quercetin occurs much easier when the molecule is bound to HSA.

3.4 Lifetime Data

Time-resolved fluorescence lifetime measurements were carried out for a sample containing a 30- μM HSA and varying (0 to 60 μM) concentrations of quercetin. The single tryptophan in HSA, *Trp214*, was selectively excited at 295 nm and fluorescence decays were collected at 340 nm. Lifetime data were initially fitted to multiexponential functions using the least-squares method. This analysis demonstrated three-exponential decays of HSA, both without and with quercetin added. The three lifetimes found for free HSA were: 0.793 ns (2.05%), 4.089 ns (44.59%), and 7.145 ns (53.35%), consistent with previous measurements.^{13,14} According to a widely accepted rotamer model, these three lifetimes can be referred to three possible conformations of tryptophan in HSA.²⁰ Numbers in brackets indicate a percentage contribution of fluorescence of each rotamer component. Adding quercetin to the system triggered changes in lifetimes and relative contributions of rotamers (see Fig. 9), but a 3-exponential nature of the decay was maintained as judged by the $\chi^2 = 1.00 \pm 0.05$ and a random distribution of residuals.

Figure 9 shows all three lifetimes decreasing with the concentration of quercetin increasing from zero to the doubled concentration of HSA. Reduction in lifetimes can be an indication of the quenching of tryptophan fluorescence by quercetin, but the already complex nature of the decay of HSA alone makes it difficult to determine which mechanism of quenching is involved, and whether it is the only process responsible for the observed changes. Indeed, quercetin-induced perturbations of the tryptophan neighborhood are likely to cause changes in fluorescence decays of the rotamers. This is supported by observed changes here in the contribution of the rotamer (B_3), which decreases with quercetin increase, while the middle-lifetime rotamer (B_2) becomes dominating. At this stage, neither quenching nor environment change can be excluded. Although a three-exponential model seems to be appropriate on the grounds of statistical criteria, it seems to be too simplistic to describe the actual kinetics.

To reveal more information on the actual excited-state kinetics of tryptophan, the raw fluorescence decays were reanalyzed and the lifetime distribution functions were determined

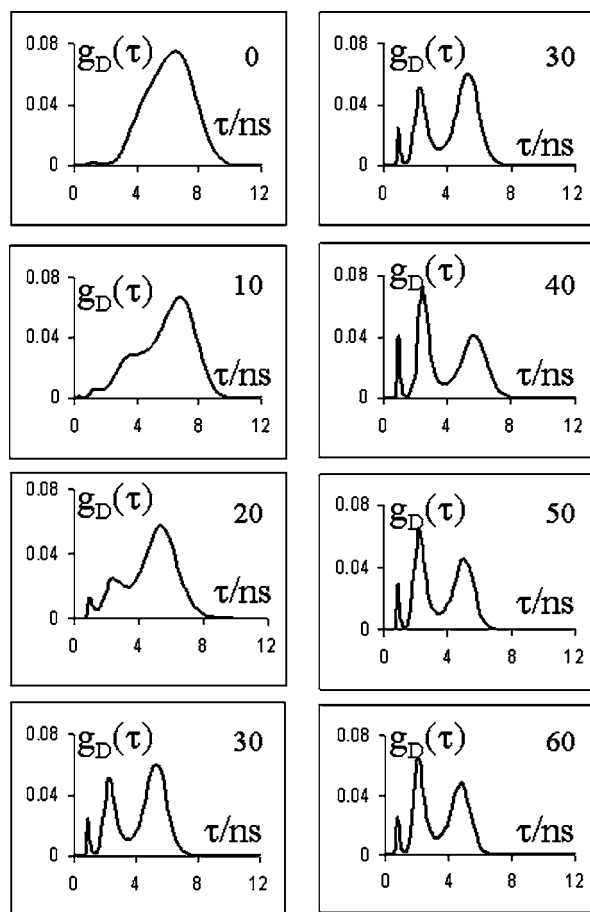


Fig. 10 Lifetime distribution functions for HSA excited at 295 nm with increasing concentrations of quercetin. The number in each plot indicates the concentration of quercetin in μM .

using software based on the maximum entropy method.¹⁶ In this approach, a simple three-exponential function would be represented by three sharp peaks on the lifetime distribution versus lifetime plot.

In our case (see Fig. 10), broad distributions of lifetimes were obtained, indicating complex kinetics of tryptophan fluorescence. For free HSA, the rotamer lifetime distribution would be expected to show three maxima, but instead of narrow peaks, broad overlapping profiles are obtained. This suggests that tryptophan can remain in a practically continuous set of configurations, and the model of three tryptophan rotamers, each characterised by a specific conformation/fluorescence lifetime, is an approximation. It seems that tryptophan in free HSA is more flexible than can be concluded from its decay fitting to a three-exponential function.

However, adding the first portion of quercetin (10 μM) results in the lifetime distribution becoming much more structured, with three well-defined peaks at 1.25, 3.34, and 6.55 ns. In our opinion, this qualitative change in the lifetime distribution profile is mainly caused by quercetin-induced structural modification of the tryptophan local environment stabilizing the range of possible tryptophan orientations, rather than by quenching, which, however, can also contribute here. Further increasing of the amount of quercetin to 20 and then to 30 μM enhances the effect of separation of the life-

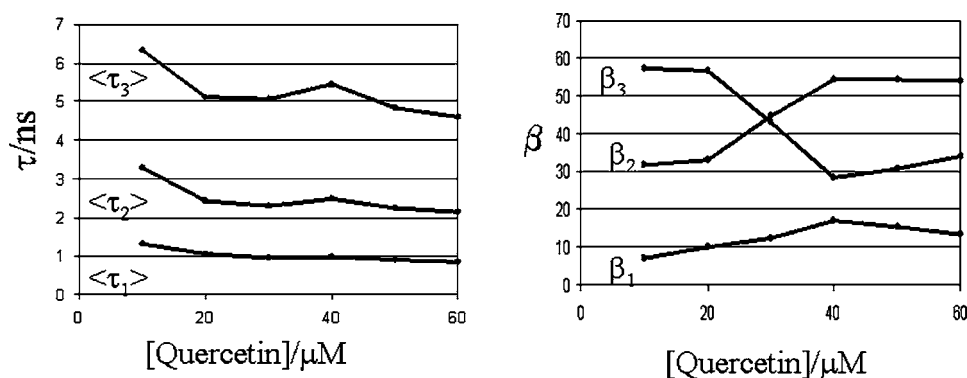


Fig. 11 Evolution of rotamer lifetimes and their contributions. The $\langle \tau_i \rangle$ and β_i parameters were obtained from fitting the lifetime distribution to the sum of Gaussian profiles.

times, but also the peak lifetimes become shorter. This observation is consistent with quercetin binding HSA at a close distance to tryptophan, which results in two processes occurring simultaneously: structural perturbation, which restricts tryptophan rotations, and quenching of tryptophan fluorescence. Effectively discrete rotamer conformation is being enhanced by the binding of quercetin.

Beginning with a 30- μM sample, the lifetime distribution functions maintain their three-peak structure, and the peak lifetimes continue to decrease with the quercetin concentration increase. The last observation suggests that at the higher concentrations of quercetin ($[\text{quercetin}] > [\text{HSA}]$), quenching starts to play a dominating role. An increased emission observed in the 490- to 550-nm section of the fluorescence spectra of the complex (Fig. 6) and relatively large $R_0 \approx 24 \text{ \AA}$ for the HSA/quercetin pair are consistent with the mechanism of this quenching being FRET. However, Fig. 10 shows also another feature of the recovered lifetime distributions: the middle-lifetime rotamer peak is monotonically increasing with quercetin, while the long-lifetime rotamer peak is decreasing (see also Fig. 11).

It seems that both perturbations in the tryptophan environment and FRET can result in the observed behavior of the decay function. In the case of environment perturbations, the middle-lifetime rotamer can gradually become more favorable than the long-lifetime rotamer. On the other hand, FRET between the long-lifetime rotamer and quercetin can be more effective due to distance or orientation-related factors. As lifetime analysis cannot distinguish between these effects, HSA-other flavonoids experiments might be helpful in confirming the suggested mechanisms.

4 Conclusion

We report steady-state and time-resolved fluorescence studies on flavonoid quercetin binding HSA. Steady-state results are consistent with the data previously reported by other authors. The novelty of our approach to HSA-flavonoid lifetime studies is based around using a new experimental opportunity, namely selective excitation of tryptophan at 295 nm and the analysis of the decays based on the maximum entropy method. The lifetime distribution functions revealed here, characterize the nature of Trp214-quercetin interactions, but cannot be interpreted in terms of a simple model. Indeed, the

fluorescence kinetics of tryptophan alone is a subject of a long-standing problem, and a rotamer model²⁰ seems to be only a good approximation of the real kinetics. In our system, tryptophan kinetics is combined with HSA-quercetin interactions, thus the precise interpretation of the resulting fluorescence responses has to be supported by additional information. In our opinion, further progress in this important aspect of nanomedical research can be stimulated by molecular dynamics, which is able to find possible locations and orientations of fluorophores attached to macromolecules, and thus help to build improved models to explain the fluorescence behavior. It would clearly be informative if a FRET analysis of donor-acceptor locations^{1,21,22} could be demonstrated in this case for HSA-quercetin.

Acknowledgments

The authors thank EPSRC and the Wolfson Foundation for financial support.

References

- O. J. Rolinski, D. J. S. Birch, L. J. McCartney, and J. C. Pickup, "Fluorescence nanotomography using resonance energy transfer: demonstration with a protein-sugar complex," *Phys. Med. Biol.* **46**(9), N221–N226 (2001).
- L. J. McCartney, J. C. Pickup, O. J. Rolinski, and D. J. S. Birch, "Near-infrared fluorescence lifetime assay for serum glucose based on allophycocyanin-labelled concanavalin A," *Anal. Biochem.* **292**(2), 212–221 (2001).
- J. C. Pickup, F. Hussain, N. D. Evans, O. J. Rolinski, and D. J. S. Birch, "Fluorescence-based glucose sensors," *Biosens. Bioelectron.* **20**(12), 2555–2565 (2005).
- C. Dufour and O. Dangles, "Flavonoid-serum albumin complexation: determination of binding constants and binding sites by fluorescence spectroscopy," *Biochim. Biophys. Acta* **1721**, 164–173 (2005).
- O. S. Wolfbeis, M. Begum, and H. Geiger, "Fluorescence properties of hydroxy- and methoxyflavones and the effect of shift reagents," *Z. Naturforsch. B* **39b**, 231–237 (1984).
- S. Ruzsnyák and A. Szent-Györgyi, "Vitamin P – flavonols as vitamins," *Nature (London)* **138**, 27 (1936).
- J. B. Harborne, "Flavonoids in the environment: structure-activity relationships," in *Plant Flavonoids in Biology and Medicine. II. Biochemical, Cellular and Medicinal Properties*, V. Cody, E. Middleton, J. B. Harborne, and A. Bertz, Eds., pp. 17–27, Allan R. Liss, New York (1988).
- B. Sengupta, A. Banerjee, and P. K. Sengupta, "Interactions of the plant flavonoid fisetin with macromolecular targets: insights from fluorescence spectroscopic studies," *J. Photochem. Photobiol., B* **80**, 79–86 (2005).

9. H. O. Gutzzeit, Y. Henker, B. Kind, and A. Franz, "Specific interactions of quercetin and other flavonoids with target proteins are revealed by elicited fluorescence," *Biochem. Biophys. Res. Commun.* **318**, 490–495 (2004).
10. A. Papadopoulou, R. J. Green, and R. A. Frazier, "Interaction of flavonoids with bovine serum albumin: a fluorescence quenching study," *J. Agric. Food Chem.* **53**, 158–163 (2005).
11. S. Bi, et al., "Investigation of the interaction between flavonoids and human serum albumin," *J. Mol. Struct.* **703**, 37–45 (2004).
12. X. M. He and D. C. Carter, "Atomic structure and chemistry of human serum albumin," *Nature (London)* **358**, 209–215 (1992).
13. C. D. McGuinness, K. Sagoo, D. McLoskey, and D. J. S. Birch, "A new sub-nanosecond LED at 280 nm: application to protein fluorescence," *Meas. Sci. Technol.* **15**(11), L19–L22 (2004).
14. C. D. McGuinness, K. Sagoo, D. McLoskey, and D. J. S. Birch, "Selective excitation of tryptophan fluorescence decay in proteins using a subnanosecond 295 nm light-emitting diode and time-correlated single-photon counting," *Appl. Phys. Lett.* **86**, 261911 (2005).
15. D. McGuinness, A. M. Macmillan, K. Sagoo, D. McLoskey, and D. J. S. Birch, "Excitation of fluorescence decay using a 265 nm pulsed light-emitting diode: Evidence for aqueous phenylalanine rotamers," *Appl. Phys. Lett.* **89**, 063901 (2006).
16. J. C. Brochon, "Maximum entropy method of data analysis in time-resolved spectroscopy," Chap. 13 in *Methods Enzymol.* **240**, pp. 262–311 (1994).
17. F. Zsila, Z. Bikadi, and M. Simonyi, "Probing the binding of the flavonoid quercetin to human serum albumin by circular dichroism, electronic absorption spectroscopy and molecular modelling methods," *Biochem. Pharmacol.* **65**, 447–456 (2003).
18. B. Mishra, A. Barik, K. I. Priyadarsini, and H. Mohan, "Fluorescence spectroscopic studies on binding of a flavonoid antioxidant quercetin to serum albumins," *J. Chem. Sci.* **117**(6), 641–647 (2005).
19. B. Sengupta and P. K. Sengupta, "The interaction of quercetin with human serum albumin: a fluorescence spectroscopic studies," *Biochem. Biophys. Res. Commun.* **229**, 400–403 (2002).
20. A. G. Szabo and D. M. Rayner, "Fluorescence decay of tryptophan conformers in aqueous solutions," *J. Am. Chem. Soc.* **102**, 2 (1980).
21. O. J. Rolinski and D. J. S. Birch, "Structural sensing using fluorescence nanotomography," *J. Chem. Phys.* **116**(23), 10411–10418 (2002).
22. O. J. Rolinski and D. J. S. Birch, "Fluorescence nanotomography: Recent progress, constraints and opportunities," Chap. 4 in *Fluorescence Spectroscopy in Biology. Advanced Methods and Their Applications to Membranes, Proteins, DNA and Cells*, M. Hof, R. Hutterer, V. Fidler, O. S. Wolfbeis, Eds., Springer Series on Fluorescence, Berlin (2005).